Journal of Fluorescence, Vol. 9, No. 4, 1999

Unraveling the Kinetic Mechanism of the 70-kDa Molecular Chaperones Using Fluorescence Spectroscopic Methods

Stephan N. Witt[1,2] and Sergey V. Slepenkov[1]

Received April 26, 1999; accepted April 27, 1999

This article reviews the recent progress in unraveling the kinetic mechanism of the 70-kDa molecular chaperones by the use of fluorescence spectroscopic methods. Dissecting the kinetics of the individual steps in the 70-kDa chaperone reaction cycle *in vitro*—ATP binding, peptide binding, interdomain coupling, and chaperone-catalyzed ATP hydrolysis—provides a foundation which can be used to develop a clear understanding of the molecular basis for chaperone activity *in vivo*.

KEY WORDS: Hsp70; chaperone; tryptophan fluorescence; environmentally sensitive fluorophores; conformational switch.

INTRODUCTION

Molecular chaperones are proteins that assist the folding, assembly, transport, and proteolysis of other proteins in nearly all biological cells [1–5]. Cells may express a plethora of different types of molecular chaperones, ranging in size from 10 to 100 kDa. This article focuses on the 70-kDa chaperones. Originally, it was discovered that when *Drosophila* cells are heat shocked they rapidly express several new proteins [6]. These inducible proteins were later aptly called heat shock proteins, and the 70-kDa protein form was termed a 70-kDa heat shock protein (Hsp70). It is now known that Hsp70 serves to renature denatured proteins and to protect native proteins from damage due to denaturation [7]. Subsequently, it was discovered that cells also constitutively express homologues of Hsp70, referred to as 70-kDa constitutive or cognate heat shock proteins (Hsc70); Hsc70 chaperones assist the folding of nascent proteins, the assembly of macromolecular complexes, and the transport of proteins across membranes and enable the proteolysis of targeted proteins. The common mechanistic feature of Hsc70 and Hsp70 chaperones is that they bind, retain, and release exposed hydrophobic segments of denatured proteins or disordered segments of native proteins in an activity cycle that depends on changes in free energy derived from the binding and hydrolysis of ATP and is regulated by the binding of cochaperones. The mechanistic details of how these chaperones discriminate between a folded protein and its unfolded form and selectively bind to the latter, and how the cycle of binding and release of the unfolded substrate to the chaperone promotes its refolding, are largely unknown.

Molecular chaperones are not protein folding catalysts because they do not accelerate the rate of folding; instead they increase the yield of the folded protein [7]. An illustration of how the 70-kDa chaperone machine might assist protein folding, which is based on the known ability of DnaK to rescue protein from aggregates [8,9], is shown in Fig. 1. An unfolded protein (U) folds into a productive intermediate (I) that possesses secondary structure but lacks well-defined tertiary structure, and the intermediate may even display hydrophobic surfaces that are normally buried in the fully folded form. The intermediate then undergoes at least three parallel reactions, each at a different rate: the intermediate misfolds (M), folds

[1] Department of Biochemistry and Molecular Biology, Louisiana State University Medical Center, 1501 Kings Highway, Shreveport, Louisiana 71130-3932.

[2] To whom correspondence should be addressed. e-mail: switt1@lsumc.edu

1053-0509/99/1200-0281$16.00/0

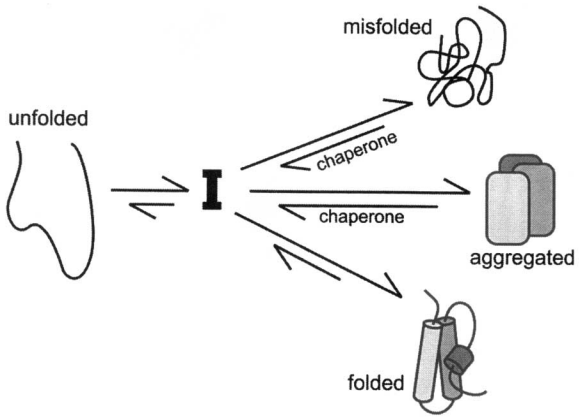

Fig. 1. Possible role of 70-kDa chaperones in protein folding. U is an unfolded protein; I is a productive intermediate; M, F, and Ag represent a misfolded protein, a folded protein, and an aggregate, respectively.

into the native state (F), and aggregates (Ag). A Hsc70 or Hsp70 chaperone probably functions as an unfoldase in that it binds to an aggregate or misfolded protein and then partially unfolds it. Put another way, the chaperone converts an unproductive dead-end species to a productive folding intermediate from which productive folding may occur. In this review, we survey the reactions between 70-kDa molecular chaperones with peptide substrates and nucleotides *in vitro* in order to establish the elementary steps in the chaperone reaction cycle, focusing here mainly on DnaK, the 70-kDa chaperone expressed by *Escherichia coli* both constitutively and under stressful conditions.

Partial proteolysis of Hsc70 and Hsp70 chaperones has revealed two functional domains: the ~44 kDa N-terminal domain binds and hydrolyzes ATP, and the ~23 kDa C-terminal domain binds polypeptide substrates. The activities of these two domains are coupled [10–13]. For example, ATP binding rather than hydrolysis induces a global conformational change in a 70-kDa chaperone molecule that tends, in general, to reduce the affinity of substrates for the polypeptide-binding domain [10,11]. Conversely, peptide binding to the C-terminal domain accelerates the rate of chaperone-catalyzed ATP hydrolysis [14–16], indicating that peptide binding promotes a conformational change in the ATPase domain of the chaperone molecule [13,17]. Because of the tendency of chaperones to aggregate, the three-dimensional structure of an intact 70-kDa chaperone has not been determined, thus the structural basis for these ligand-induced, bidirectional conformational changes is not known. On the other hand, structures of the separate functional domains have been determined.

The ATPase domain of bovine brain Hsc70 is a bilobed structure that has a deep crevice between the two lobes[18–20]. ATP, one Mg^{2+} ion and two K^+ ions bind at the base of the crevice (Fig. 2A). The global conformational change in Hsc70 and Hsp70 that is induced by the action of ATP binding is strictly dependent on K^+ in that Na^+ cannot substitute for K^+ [10]. Tryptophan residues are located in the ATPase domain of bovine brain Hsc70 and DnaK at positions 90 and 102, respectively [19,21].

The three-dimensional structure of a genetically engineered fragment of the polypeptide-binding domain of DnaK(389–607) complexed with a synthetic peptide (NRLLLTG) is shown in Fig. 2B [22–24]. Defined by two distinct subdomains, the polypeptide-binding domain consists of a β-sandwich subdomain that forms two sheets, each of which has four antiparallel β-strands and an α-helical domain, which is composed of a series of

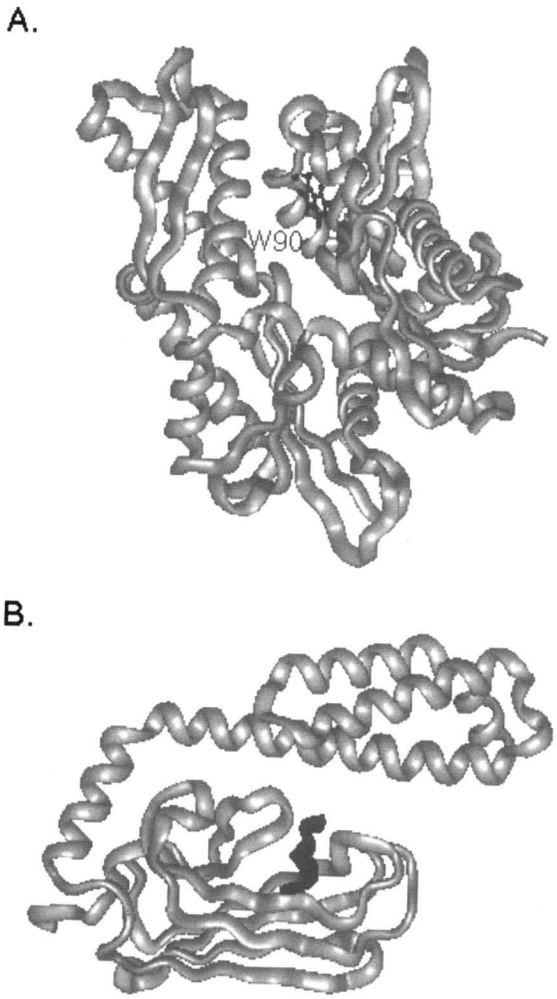

Fig. 2. **(A)** Structure of the N-terminal ATPase domain of bovine Hsc70 [18]. **(B)** Structure of a fragment of the polypeptide-binding domain of DnaK complexes with a short synthetic peptide [22]. The figure was made using files 2HSC and 1DKX from the Brookhaven Protein Data Base.

five α-helices, that possibly acts as a lid over the β-sandwich. Peptides bind in an extended conformation to loops from the β-sandwich [22,25]. This conformation, where the lidlike α-helical subdomain appears to be closed over the bound peptide, may represent the so-called high-affinity state of the polypeptide-binding domain of DnaK [22]. Note that bovine Hsc70 has one tryptophan residue in the polypeptide-binding domain at position 580 [19], whereas DnaK has no tryptophan residues in this domain.

It is well known that 70-kDa molecular chaperones bind to unfolded segments of native or nonnative proteins [26,27]. Synthetic peptides are often used as substrates in studies of molecular chaperone action because they mimic unfolded proteins [14,28]. Phage display libraries or similar combinatorial techniques have provided insight into the substrate specificity of 70-kDa chaperones [14,28–31]. The consensus from these studies is that a seven-mer is the minimal fragment necessary for binding to 70-kDa chaperones, and for DnaK, peptides that bind with the highest affinity possess a hydrophobic core, typically consisting of leucine residues, flanked by basic residues. Peptides derived from combinatorial libraries are often referred to as chaperone substrates, but they are not true substrates since they have no physiological relevance. Based on equilibrium studies [29,32], one molecule of synthetic peptide binds per chaperone molecule; presumably physiological substrates also bind in a 1:1 stoichiometry (Fig. 2B).

ATP-INDUCED CHANGES IN THE TRYPTOPHAN FLUORESSENCE OF DnaK

A key finding, which has led to numerous kinetic studies, as described below, was that ATP induces a global conformational change in a Hsp70 or Hsc70 chaperone molecule. This finding came about from fluorescence experiments that demonstrated that the addition of excess ATP to a solution of DnaK induces a rapid reduction in the intrinsic tryptophan fluorescence and a concomitant blue-shift in the emission maximum from 335 to 320 nm [10,33]. An illustration of the effect of ATP on the fluorescence spectrum of DnaK is shown in Fig. 3. Other nucleotides, such as ADP, or nonhydrolyzable ATP analogues, such as AMP-PNP, do not quench the fluorescence of the 70-kDa chaperones. The presence of the γ-phosphate group of ATP is thus absolutely necessary to induce the conformational change. Iodide quenching experiments have shown that the tryptophan is less exposed to solvent after the addition of ATP [34]. Protease digestion and small-angle x-ray scattering experiments have confirmed and extended these fluorescence experiments [12,35,36]. This ATP-induced conformational change in a 70-kDa molecule is represented as

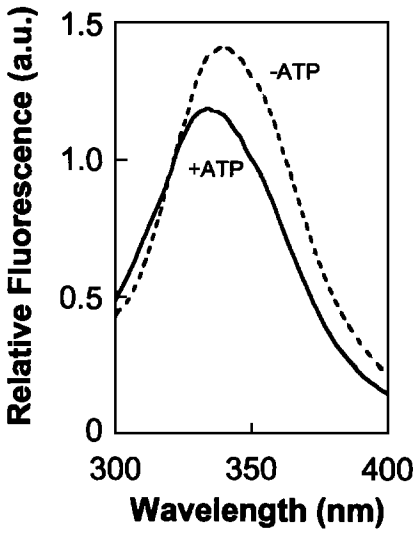

Fig. 3. Effect of ATP on the fluorescence spectrum of DnaK. Fluorescence emission spectra of DnaK with and without ATP. Conditions: [DnaK] = 1.0 μ*M*; [ATP] = 1.0 m*M*; temperature = 25°C; λ_{ex} = 295 nm; excitation bandwidth = 3.0 nm; emission bandwidth = 5 nm. Reprinted with permission from Ref. 41. Copyright 1998 American Chemical Society.

$$\text{ATP} + \text{E} \Leftrightarrow \text{ATP–E}^* \quad (1)$$

where E and ATP–E* represent the high- and low-affinity states of DnaK [10], respectively, and the asterisk denotes a state with reduced fluorescence relative to the E state. In general, the high-affinity state tightly binds substrates, and the low-affinity state weakly binds substrates [10,11]. The time course for the formation of DnaK–peptide complexes in the absence or presence of ATP in Fig. 4 illustrates the differential reactivity of the high-affinity and low-affinity states toward a peptide. Possible structural changes that occur during this ATP-induced conformational change are discussed below.

Because nucleotide triphosphates but not diphosphates induce the E → E* transition, it was assumed that the hydrolysis of ATP brings about the conformational transition. This is not the case, because when ATP is added to DnaK–RCMLA complexes (RCMLA, reduced carboxymethylated lactalbumin, is a permanently unfolded form of lactalbumin) the bound RCMLA dissociates within seconds, whereas the ATP was hydrolyzed in minutes [10]. Thus, Palleros and co-workers concluded that the ATP-induced conformational change in DnaK is due to ATP binding rather than hydrolysis [10]. The same investigators found that the ATP-induced conformational change is dependent on the presence of potassium ions.

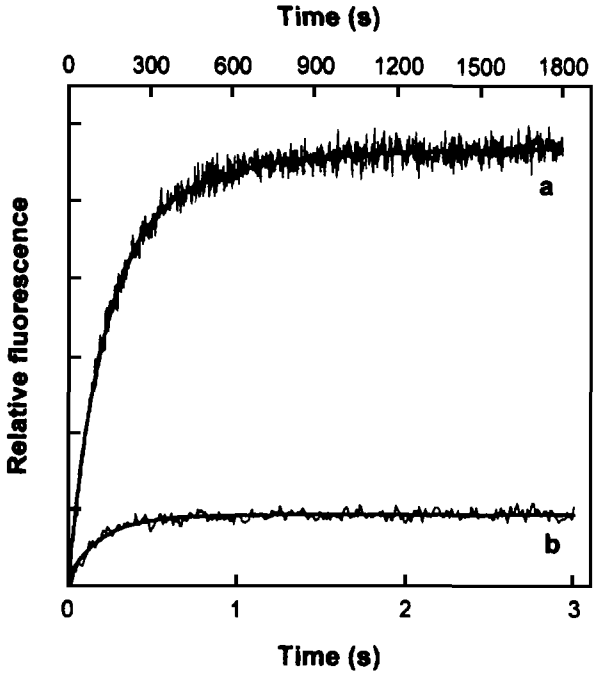

Fig. 4. DnaK–peptide complex formation in the absence or presence of ATP. Curve a, DnaK–fluorescent–peptide complex formation in the absence of nucleotide. Curve b, DnaK–fluorescent–peptide complex formation in the presence of ATP. Conditions: peptide = a-CLLLSAPRR (a, acrylodan); λ_{ex} = 370 nm; λ_{em} = 500 nm; temperature = 25°C; final concentrations in a and b were 50 n*M* a-peptide and 1 μ*M* DnaK. This figure was taken from Ref. 60 and printed with the permission of Academic Press LTD.

Because DnaK hydrolyzes ATP with a steady-state turnover number of only 0.0003 s^{-1} at 25°C, and because the same value is obtained in single-turnover experiments [37], neither a rapid burst of ATP hydrolysis nor phosphate transfer plays any significant role in the chaperone reaction cycle in the absence of protein substrate and cochaperones. Hsp70 and Hsc70 chaperones are similar to G-proteins because both slowly hydrolyze nucleotide triphosphates [10,37].

Terms used in this article are defined as follows. As shown above, E → E* (or T + E → TE*) represents the high-to-low-affinity conformational change in a 70-kDa chaperone molecule, where intermediates are ignored. The reverse reaction, the low-to high-affinity conformational change, is represented as E* → E. An ~15% *decrease* in tryptophan fluorescence of the chaperone molecule occurs as a consequence of the E → E* conformational change, whereas an ~15% *increase* in tryptophan fluorescence of the chaperone molecule occurs as a consequence of the E* → E conformational change. Note that the hydrolysis of chaperone-bound ATP often accompanies the E* → E reaction. The sequence of the two reactions—the E* → E conformational change and the hydrolysis of bound ATP—is discussed at length below.

KINETICS OF THE HIGH- TO LOW-AFFINITY STRUCTURAL TRANSITION (E → E*)

The kinetic mechanism of the conformational coupling between the two functional domains—how a conformational change is transmitted from the ATPase domain upon ATP binding to the substrate-binding domain—has been investigated using stopped-flow fluorescence techniques [38–43]. In such experiments, the rapid reduction in tryptophan fluorescence is monitored upon mixing ATP with either nucleotide-free chaperone molecules or chaperone–peptide complexes (ATP + E or ATP + EP).

When ATP is rapidly mixed with nucleotide-free bovine Hsc70, the tryptophan fluorescence of the chaperone is quenched with biphasic kinetics [38]. Plots of the apparent first-order rate constants for the fast and slow phases versus [ATP] were linear and hyperbolic, respectively. These results were interpreted according to the two-step sequential reaction shown in Scheme I.

$$\mathrm{ATP} + \mathrm{E} \underset{k_{-1}}{\overset{k_1}{\Leftrightarrow}} \mathrm{ATP\text{-}E} \underset{k^*_{-1}}{\overset{k^*_1}{\Leftrightarrow}} (\mathrm{ATP\text{-}E})^*$$

Scheme I

ATP binding occurs in the first step and a conformational transition occurs in the second step. E represents nucleotide-free Hsc70, ATP–E is a transient, and (ATP–E)* is the low-affinity state. Estimates for the rate constants are $k_1 = 7 \times 10^5\ M^{-1}\ s^{-1}$, $k_{-1} = 1.1\ s^{-1}$, $k_1^* \approx 0.66\ s^{-1}$, and $k_{-1}^* \approx 0.02\ s^{-1}$ [38]. The overall binding of ATP to Hsc70 is very tight ($K_d^1 \times K_d^* = 0.042 \pm 0.007\ \mu M$). Similar experiments on nucleotide-free DnaK have revealed a biphasic reduction in the tryptophan fluorescence of DnaK [41,42], although the results were interpreted in terms of a three-step sequential reaction with a preequilibrium between two different DnaK species [41].

It is well known that peptide binding to the C-terminal domain of a chaperone molecule increases the steady-state rate of DnaK-catalyzed ATP hydrolysis [14–16]; thus, it is reasonable to conclude that peptide binding to DnaK alters the structure of the ATPase domain, which in turn facilitates the hydrolysis of ATP. To probe the role of a bound peptide on the reactivity of the ATPase domain, recent studies have probed the pre-steady-state kinetics of ATP binding to nucleotide-free, high-affinity

DnaK–peptide complexes [40,43]. The traces in Fig. 5A were obtained from such an experiment. Specifically, ATP (0–1000 μM) was mixed with a fixed concentration of nucleotide-free DnaK–Cro peptide complexes, where the Cro peptide (MQERITLKDYAM) mimics an unfolded substrate. (The Cro peptide binds to nucleotide-free DnaK with an equilibrium dissociation constant K_d = 7 μM [44]). The traces follow single-exponential kinetics,

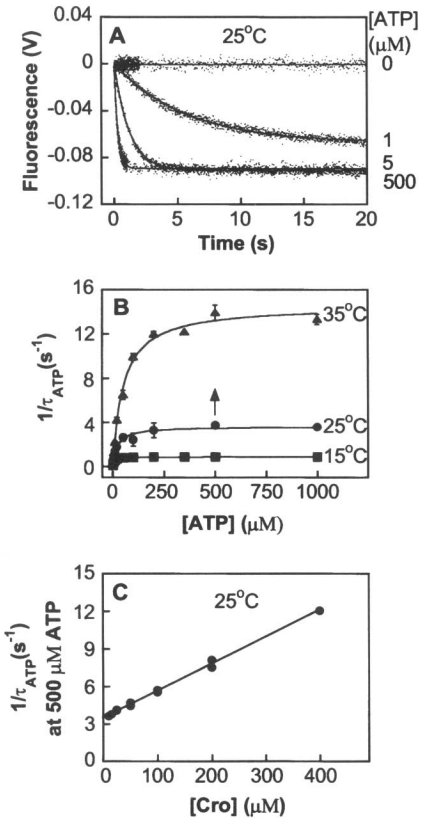

Fig. 5. (**A**) Kinetics of ATP-induced decrease in the tryptophan fluorescence of DnaK–Cro peptide complexes monitored by stopped-flow fluorescence. Traces follow $F(t) = \Delta F e^{-t/\tau_{ATP}} + F_\infty$ (solid lines), with rates, $1/\tau_{ATP}$, equal to 0.18, 0.80, and 3.6 s^{-1} at 1, 5, or 500 μM ATP, respectively. Conditions: Final concentrations after mixing were 1.0 μM DnaK and 20 μM Cro; temperature = 25°C. V is volts. (**B**) Plots of the rate ($1/\tau_{ATP}$) versus [ATP] at a constant Cro concentration (20 μM). Data points are the average of two or three determinations conducted on different days. Data are fit to $1/\tau_{ATP} = k_{on}[P] + (k_{off}[ATP]/(K_1 + [ATP]))$ (solid lines) [43]. The asymptote of each plot equals $k_{on}[P] + k_{off}$. The vertical arrow above the points at 500 μM ATP (25°C) indicates that the asymptote increases with increasing concentrations of Cro peptide. (**C**) Plot of the reciprocal relaxation time for the fluorescence decrease ($1/\tau_{ATP}$) (●) versus [Cro] at constant ATP (500 μM). The slope and y-intercept are k_{on} (2.1 ± 0.1 × 10^4 M^{-1} s^{-1}) and k_{off} (3.5 ± 0.1 s^{-1}), respectively. Final concentrations after mixing were 1 μM DnaK, 10–400 μM Cro, and 500 μM ATP; temperature = 25°C. Reprinted with permission from Ref. 43. Copyright 1998 American Chemical Society.

$F(t) = \Delta F \exp(-t/\tau_{ATP}) + F_\infty$, and over a range of temperatures the reciprocal relaxation time of the ATP-induced reduction in the tryptophan fluorescence of DnaK, $1/\tau_{ATP}$, exhibits a hyperbolic dependence on the concentration of ATP [40,43]. A unique aspect of the reaction between ATP and DnaK–peptide complexes is that the asymptote of the plot of $1/\tau_{ATP}$ vs [ATP] in Fig. 5B is not a constant; instead, the numerical value of the asymptote increases with increasing concentrations of the Cro peptide (Fig. 5C) [43]. These combined results are consistent with the minimal mechanism shown in Scheme II,

$$\begin{array}{ccccc} & & E & & \\ & & + & & \\ & & P & & \\ & & \uparrow\downarrow & K_1 & k_{off} \\ \mathbf{ATP} & + & \mathbf{EP} & \Leftrightarrow \mathbf{ATP\text{-}EP} & \Leftrightarrow \mathbf{ATP\text{-}E^*} + \mathbf{P} \\ & & & & k_{on} \end{array}$$

Scheme II

where EP is a high-affinity DnaK–peptide complex, ATP–EP is a high-affinity intermediate complex, ATP–E* is the low-affinity form of DnaK, and the ATP–E* state has reduced fluorescence relative to EP and ATP–EP complexes. ATP binding and dissociation occur in the first step and a structural switch occurs in the second step. At 25°C, K_1, k_{on}, and k_{off} equal 22 μM, 2.1 ± 0.1 × 10^4 M^{-1} s^{-1}, and 3.4 ± 0.5 s^{-1}, respectively. The equilibrium dissociation constant for the structural switch in the presence of the Cro peptide is 162 μM ($K_d = k_{off}/k_{on}$).

Because the numerical values for both the second-order rate constant for ATP binding to nucleotide-free DnaK ($k_1 \approx 1 \times 10^5$ M^{-1} s^{-1}) and the second-order rate constant for Cro peptide binding to low-affinity DnaK ($k_{on} = 2.1 \times 10^4$ M^{-1} s^{-1}) are much less than the value expected for a diffusion controlled reaction ($k \sim 10^9$ M^{-1} s^{-1}), transients probably form very quickly upon the addition of ATP to nucleotide-free, high-affinity DnaK or upon the addition of peptide to low-affinity DnaK [37,41].

The structure in Fig. 2B shows that the chaperone-bound peptide is lodged within a deep channel that is topped by an α-helical lidlike subdomain; this molecular complex is probably the "high-affinity chaperone–peptide complex." Of course, *in vivo*, much larger polypeptides must fit into the binding site. An intriguing question is, if the lid blocks the polypeptide binding site, how do polypeptide substrates get in and out of the binding site? One proposal is that ATP binding to the chaperone molecule triggers the lid to open [22]. Extending this idea, Scheme II can be reformulated as ATP + E_cP ⇔ ATP–E_cP ⇔ ATP–E_o^* + P, where c and

o denote closed and open states of the chaperone's C-terminal domain. The peptide dissociation experiments, discussed below, are consistent with such a structural model.

MECHANISM OF CHAPERONE–PEPTIDE COMPLEX DISSOCIATION

Several studies have probed the kinetics and mechanism of chaperone–peptide complex formation and dissociation using synthetic peptides tagged with environmentally sensitive fluorophores [11,39,42,43, 45,46]. Regarding chaperone–peptide complex dissociation, these studies have revealed the remarkably different rates of peptide release from DnaK, depending on which nucleotide is present, ADP or ATP. In most but not all cases, ATP significantly accelerates the rate of peptide release from preformed 70-kDa chaperone–peptide complexes. The huge effect of ATP on the rate of peptide release from DnaK is illustrated by the case of the Cro peptide. The dissociation of the Cro peptide from DnaK in the presence of ADP or ATP is shown in Fig. 6. At 25°C, the apparent first-order rate constant for the dissociation of Cro from DnaK is $1.2 \pm 0.2 \times 10^{-4}$ and $3.3 \pm 0.1\ s^{-1}$ in the presence of ADP and ATP, respectively, and the activation enthalpies for Cro dissociation

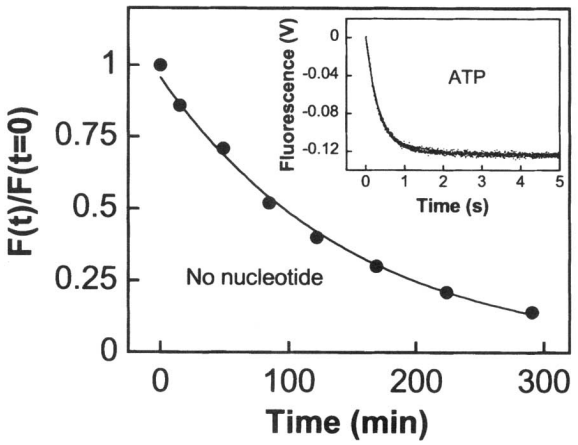

Fig. 6. Kinetics of fCro peptide dissociation from preformed DnaK–fCro complexes. (●) The dissociation of fCro from preformed DnaK–fCro complexes in the absence of nucleotide monitored by size-exclusion chromatography. The dissociation follows single-exponential kinetics (solid line), with $k_{off}^{app} = 1.2 \times 10^{-4}\ s^{-1}$. Inset: The dissociation of fCro from preformed DnaK–fCro complexes upon mixing with ATP monitored by stopped-flow fluorescence. The dissociation follows single-exponential kinetics, with $k_{off}^{app} = 3.3\ s^{-1}$. Conditions: temperature = 25°C; 1–2 μ*M* DnaK–fCro complexes (f = dansyl group at the N terminus); 1 m*M* ATP; ~30 μ*M* unlabeled Cro was mixed with the complexes at time 0.

in ADP and ATP are 34.6 ± 1 and 23 ± 2 kcal mol^{-1}, respectively [43,44]. Thus, ATP accelerates the rate of Cro peptide release from DnaK by a factor of nearly 30,000. The huge activation enthalpy and slow rate of Cro peptide dissociation from DnaK in the presence of ADP are probably due to an uncatalyzed high- to low-affinity transition in an ADP–DnaK–peptide complex that precedes peptide release, rather than simple peptide dissociation (EP→E+P). Such a reaction is depicted below.

$$\text{ADP–E}_c\text{P} \overset{\text{slow}}{\rightarrow} \text{ADP–E}_o^*\text{P} \overset{\text{fast}}{\rightarrow} \text{ADP–E}_o^* + \text{P} \quad (2)$$

where ADP–E_cP is a high-affinity complex in which the lid is closed (see Fig. 2B), ADP–E_o^*P is a low-affinity intermediate in which the lid is open, ADP–E_o^* is the low-affinity form of DnaK, and the asterisk denotes reduced fluorescence relative to the high-affinity state. We surmise that the value of $\Delta H^{\ddagger} = 34$ kcal mol^{-1}, determined for fCro (fCro, N-terminally labeled Cro peptide) dissociation from preformed high-affinity complexes, is due to the first step in reaction (2), the $E_c \rightarrow E_o^*$ switch. ATP binding catalyzes this switch, as we have shown, leading to a significant reduction in the activation enthalpy barrier ($\Delta H^{\ddagger} = 23$ kcal mol^{-1}); however, even in the presence of ATP the transition still precedes and therefore limits the rate of peptide dissociation. This explains why there is so little variation in peptide off-rates when ATP is added to preformed chaperone peptide complexes [42,47]. In this vein, note that the apparent first-order rate constant for fCro peptide dissociation from preformed DnaK–fCro complexes in the presence of ATP ($k_{off}^{app} = 3.3 \pm 0.1\ s^{-1}$) equals the value of the first-order rate constant for the E → E* transition ($k_{off} = 3.4 \pm 0.5\ s^{-1}$), determined from experiments which followed the reduction in the intrinsic tryptophan fluorescence of DnaK–Cro peptide complexes (Fig. 5).

THE LOW- TO HIGH-AFFINITY TRANSITION (E* → E) WITH ATP HYDROLYSIS

Due to the high-affinity binding of ATP to DnaK, DnaK exists predominantly in the low-affinity form under conditions where there is an excess of ATP over ADP (such as in a biological cell). If the low-affinity chaperone state predominates in a cell and the low-affinity form weakly binds nonnative substrates, how does polypeptide binding to the low-affinity chaperone state bring about conversion to the high-affinity state? A variety of fluorescence studies has addressed this question by examining

the kinetics, mechanism, and catalysis of the low- to high-affinity conformational change.

The kinetics of the low- to high-affinity conformational transition in DnaK (E* → E) in the absence of peptide substrate and under single-turnover conditions ([DnaK] = [ATP]) are intriguing because the reaction is unusually slow, occurring with a half-time of ~20 min at room temperature; the reaction is so slow that it must be catalyzed *in vivo*. The E* → E transition in the absence of peptide or cochaperone is readily studied by mixing DnaK and ATP and monitoring the changes in fluorescence in real time using a fluorometer in the time base mode [38,40,41]. Addition of a stoichiometric amount of ATP to DnaK induces a biphasic change in the tryptophan fluorescence (Fig. 7): after the rapid initial decrease in fluorescence the signal gradually returns to its initial value. The rapid initial decrease in fluorescence is the two-step E → E* transition; the slow increase in fluorescence is the E* → E transition. The traces follow single-exponential kinetics, with an observed first-order rate constant k_{obs} equal to $1.4 \pm 0.1 \times 10^{-4}$ and $1.5 \pm 0.1 \times 10^{-3}$ s^{-1} at 20 and 37°C, respectively. For comparison, the steady-state rate of DnaK-catalyzed ATP hydrolysis k_{cat} equals $2.7 \pm 0.7 \times 10^{-4}$ and 1.5×10^{-3} s^{-1} at 22 and 37°C, respectively [44,48]. The similarity between these k_{obs} values for the E* → E fluorescence transition and the k_{cat} values indicates that ATP hydrolysis by DnaK may be the rate-limiting step in the E* → E transition. This interpretation and others are discussed below.

Consider the following mechanisms for the linkage between ATP hydrolysis and the E* → E transition. First, suppose that ATP hydrolysis and the low- to high-affinity conformational change occur in a single step, according to

$$\text{ATP–E*} \xrightarrow{\text{slow}} \text{ADP–E} \qquad (3)$$

Such a reaction seems improbable because it is unlikely that the hydrolysis of bound ATP could occur at precisely the same instant as the conformational change in the protein. Second, suppose that DnaK-catalyzed ATP hydrolysis is rate-limiting and precedes the conformational change [reaction (4)] [38,40,41].

$$\text{ATP–E*} \xrightarrow[k_{hy}]{\text{slow}} \text{ADP–E*} \overset{\text{fast}}{\Leftrightarrow} \text{ADP–E} \qquad (4)$$

In the above reaction, free energy from the hydrolysis of ATP is used to do work—change the conformation of the protein in the DE*→DE reaction, where D stands for ADP. Third, suppose that the low- to high-affinity conformational change in DnaK is rate-limiting and precedes the hydrolysis of bound ATP [reaction (5)] [37,49].

$$\text{ATP–E*} \overset{\text{slow}}{\Leftrightarrow} \text{ATP–E} \xrightarrow[k_{hy}]{\text{fast}} \text{ADP–E} \qquad (5)$$

In the above reaction, the hydrolysis of ATP to ADP is used to do physical work, i.e., either change the conformation of DnaK or change the conformation of the bound substrate after ATP hydrolysis in a reaction distinct from TE* → TE. While the above reactions are theoretically possible, experiments, described below, indicate that the low- to high-affinity conformational change is rate-limiting and precedes the hydrolysis of DnaK-bound ATP according to reaction (5). Thus, we suggest that the large activation enthalpy barrier ($\Delta H^{\ddagger} \approx 26$ kcal mol^{-1}) measured under single turnover conditions for both the E* → E fluorescence transition (Fig. 7) and DnaK-catalyzed ATP hydrolysis is due to the low- to high-affinity TE* → TE conformational change in DnaK [37,41], where T stands for ATP.

One other point regarding reactions (3)–(5) should be made. It was discussed above that peptide binding to the C-terminal domain of the chaperone stimulates the hydrolysis of ATP by the chaperone. It is difficult to explain the phenomenon that peptide binding stimulates chaperone-catalyzed ATP hydrolysis by reaction (3) or (4) because in those two reactions peptide binding is not linked to ATP hydrolysis by the chaperone. On the other hand, reaction (5) can, in theory, explain the effect of peptide on chaperone-catalyzed ATP hydrolysis because there is a conformational change *prior* to ATP hydrolysis that is catalyzed by peptide binding, and this conforma-

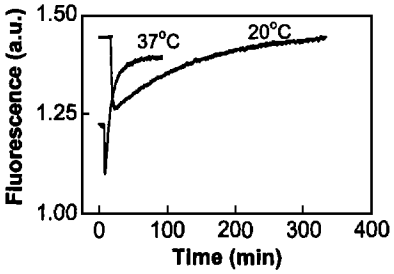

Fig. 7. Kinetics of the low- to high-affinity switch (E* → E) under single-turnover conditions in the absence of peptide. The formation portion of each trace follows the equation $F(t) = \Delta F(1 - \exp(-k_{obs}\, t)) + \gamma$ (solid lines), where ΔF, k_{obs}, and γ are the amplitude, the first-order observed rate constant, and the fluorescence at the time 0 point, respectively. The best-fit equations are as follows: 20°C, $F(t) = 2.3 \times 10^5 (1 - \exp(-0.00014\ s^{-1}\, t)) + 1.2 \times 10^6$; and 37°C, $F(t) = 6.6 \times 10^5 (1 - \exp(-0.0015\ s^{-1}\, t)) + 7.3 \times 10^5$. Conditions: $\lambda_{ex} = 295$ nm (bandwidth = 3 nm); $\lambda_{em} = 340$ nm (bandwidth = 5 nm). Reprinted with permission from Ref. 41. Copyright 1998 American Chemical Society.

tional change is likely to alter the environment surrounding the ATP binding site in such as way as to promote the hydrolysis of ATP.

PEPTIDE-INDUCED CHANGES IN THE TRYPTOPHAN FLUORESCENCE OF DnaK: PROMOTION OF THE LOW- TO HIGH-AFFINITY CONFORMATIONAL CHANGE (E* → E) BY PEPTIDE BINDING

The effect of peptide substrate on the kinetics of the low-to-high-affinity conformational transition in DnaK were recently probed by monitoring changes in the intrinsic tryptophan fluorescence of DnaK [43]. The traces in Fig. 8A show that (i) the rapid mixing of low-affinity DnaK complexes with excess Cro peptide induces a rapid increase in tryptophan fluorescence (ATP–E* + P); (ii) mixing excess Cro with DnaK causes no change in tryptophan fluorescence (E + P); and (iii) mixing ATP with preformed DnaK–Cro complexes induces a decrease in fluorescence (ATP + EP). The results reveal that the presence of excess Cro peptide rapidly shifts low-affinity DnaK complexes to high-affinity complexes, resulting in an increase in tryptophan fluorescence, consistent with Scheme II. In other words, the above results suggest that the Cro peptide catalyzes the TE* → TE transition prior to the hydrolysis of ATP (compare Figs. 8A and 7).

If the Cro peptide catalyzes the low- to high-affinity switch in the structure of DnaK, which is the reverse of the second step in Scheme II (P + ATP–E* ⇔ ATP–EP), the second- and first-order rate constants for this reaction should be exactly equal to the values for these constants that were obtained from experiments where ATP was mixed with high-affinity DnaK–peptide complexes (k_{on} = 2.1 ± 0.1 × 10^4 M^{-1} s^{-1} and k_{off} = 3.4 ± 0.5 s^{-1}; Fig. 5C). To ascertain values for these rate constants, the reaction between low-affinity DnaK and unlabeled Cro peptide was examined by varying the peptide concentration at a fixed concentration of low-affinity DnaK (Fig. 8B) [43]. The fluorescence traces follow single-exponential kinetics, $F(t) = \Delta F\,(1 - \exp[-t/\tau_{Cro}]) + F_o$, and the plots of the reciprocal relaxation time $1/\tau_{Cro}$ vs Cro peptide concentration are linear, with the slope and *y*-intercept equal to k_{on} (2.4 ± 0.4 × 10^4 M^{-1} s^{-1}) and k_{off} (2.9 ± 0.5 s^{-1}) (Fig. 8C), respectively. These values agree within the experimental uncertainty with values for k_{on} and k_{off} determined from experiments where ATP was mixed with high-affinity DnaK–peptide complexes (compare Figs. 5C and 8C). Such results strongly indicate that the structural switch is reversible.

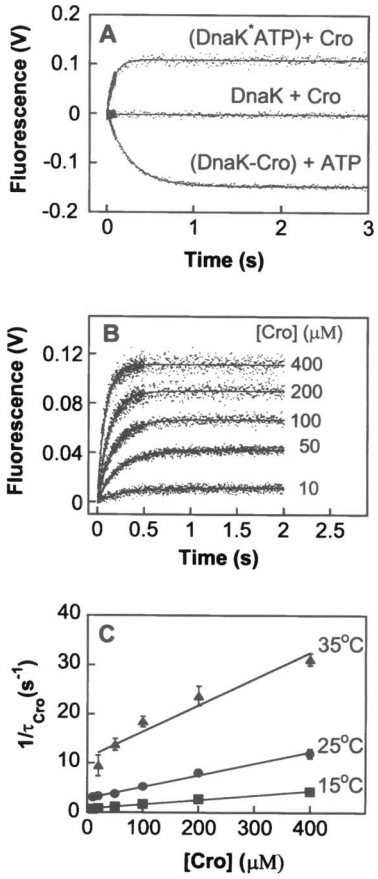

Fig. 8. (**A**) Comparison of the changes in the tryptophan fluorescence of DnaK due to three reactions: (i) Cro + low-affinity DnaK complexes (top trace); (ii) Cro + DnaK (middle trace); and (iii) ATP + DnaK–Cro complexes (bottom trace). Final concentrations after mixing were (i) 1 μ*M* DnaK, 400 μ*M* Cro, and 500 μ*M* ATP; (ii) 1 μ*M* DnaK, 400 μ*M* Cro; and (iii) 1 μ*M* DnaK, 20 μ*M* Cro, and 500 μ*M* ATP. (**B**) Kinetics of the Cro peptide-induced increase in the tryptophan fluorescence of low-affinity DnaK complexes (Cro + ATP–E*). Traces follow $F(t) = \Delta F(1 - e^{-t/\tau_{Cro}}) + F_o$ (solid line), with rates $1/\tau_{Cro}$ equal to 3.3, 4.2, 5.4, 7.5, and 11.5 s^{-1} at 10, 50, 100, 200, and 400 μ*M* Cro. Temperature = 25°C; 500 μ*M* ATP. (**C**) Plots of $1/\tau_{Cro}$ versus [Cro]. Data were fit to $1/\tau_{Cro} = k_{on}[Cro] + k_{off}$ (solid lines). Values for k_{on} and k_{off} are listed in Table I. Reprinted with permission from Ref. 43. Copyright 1998 American Chemical Society.

The TE* → TE transition occurs with a reciprocal relaxation time of 30 s^{-1} in the presence of 400 μ*M* Cro peptide at 35°C (Fig. 8C), whereas DnaK hydrolyzes ATP with a steady-state rate k_{cat} equal to 0.0086 ± 0.0032 s^{-1} in the presence of 400 μ*M* Cro at 37°C [44]. This huge disparity in rates suggests that the low- to high-affinity conformational switch in DnaK *precedes* ATP hydrolysis, according to reaction (5). Rate constants for Cro peptide release from preformed DnaK–Cro complexes, derived from three experiments (Figs. 5, 6, and 8) are given in Table I.

Table I. Reaction of DnaK with the Cro Peptide

Reaction[a]	Rate constant	$\Delta H^{\ddagger}$ (kcal mol^{-1})	
$P + E \overset{k_{on}}{\rightarrow} EP$	k_{on}: 18 ± 5 M^{-1} s^{-1}	26 ± 8	Ref. 44
$EP \overset{k_{off}}{\rightarrow} E + P$	k_{off}: 1.2 ± 0.2 10^{-4} s^{-1}	34.6 ± 1.2	Fig. 6
$T + EP \Leftrightarrow TEP \underset{k_{on}}{\overset{k_{off}}{\Leftrightarrow}} TE^* + P$	k_{off}: 3.4 ± 0.5 s^{-1} k_{on}: 2.1 ± 0.1 × 10^4 M^{-1} s^{-1}	Off: 23 ± 1 On: 15 ± 1	Fig. 5
$T + EfP \overset{k_{off}}{\Leftrightarrow} TE^* + fP$	k_{off}: 3.3 ± 0.1 s^{-1}	23 ± 1	Fig. 6
$P + TE^* \underset{k_{off}}{\overset{k_{on}}{\Leftrightarrow}} TEP$	k_{off}: 2.9 ± 0.5 s^{-1} k_{on}: 2.4 ± 0.4 × 10^4 M^{-1} s^{-1}	23 ± 1 15 ± 1	Fig. 8

[a] EP denotes a high-affinity DnaK–peptide complex; P denotes the Cro peptide.

REACTION OF FLOURESCENT PEPTIDES WITH PREFORMED LOW-AFFINITY DnaK COMPLEXES (P + ATP–E* ⇔ ATP–E*–P)

Recent studies have investigated the binding of a panel of seven different synthetic peptides to low-affinity DnaK complexes [42,47]. The peptides were tagged with the environmentally sensitive fluorophore, acrylodan, which enabled DnaK–peptide complex formation to be monitored in real time by following the changes in acrylodan fluorescence upon complex formation. The changes in tryptophan fluorescence of DnaK were not monitored. In these stopped-flow experiments, the fluorescent peptide concentration was fixed (100 nM) and the concentration of low-affinity DnaK complexes was varied (1–22 μM). Depending on the sequence of the peptide, the peptides bind to low-affinity DnaK complexes with either single- or double-exponential kinetics, and the magnitudes of the first- and second-order rate constants vary considerably with peptide sequence (Table II). For example, the second-order rate constant k_{p1} for peptide binding varies from 44 to 1.1 × 10^6 M^{-1} s^{-1}, while the first-order rate constant for peptide release k_{p-1} varies from 0.004 to 7.2 s^{-1} (see Scheme III). Complementary experiments monitored the dissociation of these same peptides from preformed DnaK–peptide complexes upon mixing with ATP; the apparent first-order dissociation rate constants (k_{off}^{app}) from these experiments exhibits much less variability (2.2–6.7 s^{-1}) (Table II). Note that for several of the peptides examined, $k_{p-1} \neq k_{off}^{app}$.

On the basis of the above results, it was proposed that there are two low-affinity forms of DnaK, one form is transient and the other is stable [42]. Transient low-affinity complexes persist for a second or less after mixing ATP with DnaK and lead to stable or equilibrium low-affinity complexes, which persist for several minutes. A model for chaperone–peptide complex formation and dissociation that incorporates these two forms of low-affinity DnaK is shown in Scheme III [42].

$$ATP + EP \overset{k_{off}^{app}}{\rightarrow} \{ATP\text{-}E^*\}_i + P$$

$$\{ATP\text{-}E^*\}_i \rightarrow ATP\text{-}E^*$$

$$P + ATP\text{-}E^* \underset{k_{p-1}}{\overset{k_{p1}}{\Leftrightarrow}} ATP\text{-}E^*\text{-}P \underset{k_{p-2}}{\overset{k_{p2}}{\Leftrightarrow}} ATP\text{-}E^*\text{-}P$$

Scheme III

In the first reaction in Scheme III, the binding of ATP to a high-affinity DnaK–peptide complex triggers a global conformational change yielding in a low-affinity transient and free peptide. This ATP-induced release of the bound peptide is like a catapult, and the reaction is unidirectional because transient complexes isomerize (second reaction in Scheme III), which prevents rebinding. Thus, when stopped-flow experiments are conducted by mixing fluorescent peptide with preformed low-affinity DnaK complexes, peptides bind according to the third reaction in Scheme III, and, depending on the sequence of the peptide, a peptide can bind to equilibrium low-affinity DnaK complexes (ATP–E*) with single- or double-exponential kinetics. The magnitudes of k_{p1} and k_{p-1} are thus peptide sequence-dependent. In contrast, k_{off}^{app} exhibits almost no dependence on the sequence of the peptide because it reflects a conformational change in the chaperone molecule [42]. The significance of this "catapult" mechanism is that there are two peptide release

Table II. Rate Constants for the Reaction Between Peptides and the Low-Affinity Form of DnaK (P + ATP–E* → ATP–E*–P)

Peptide	k_{p1} (M^{-1} s^{-1})	k_{p-1} (s^{-1})	k_{p2} (M^{-1} s^{-1})	k_{p-2} (s^{-1})	(ATP + EP → ATP–E* + P), k_{off}^{app} (s^{-1})
a-pp	450,000	1.8			2.6 ± 0.26
a-p4	55,000	7.2	0.8	0.3	5.5 ± 1.3
a-p5	1,115,000	5.7			6.7 ± 1.2
a-p6	44	0.0004			5.6 ± 0.035
a-NR	104,000	4.5	0.016	0.018	5.4 ± 0.0057
a-$(LS)_4$	96	0.04			2.4 ± 0.1
a-pσ^{32}	210	0.013	0.001	0.0005	0.9 ± 0.004

[a] a-pp, a-CALLQSRLLLSAPRRAAATARA; a-p4, CALLQSRLLS; a-p5, A-CLLLSAPRR; a-p6; a-CARSLLLSS; a-NR, a-NRLLLTG; a-$(LS)_4$, a-LSLSLSLS; a-pσ^{32}, a-QRKLFFNLRKTKQ; a, acrylodan. This is reprinted from Ref. 42 with the permission of Academic Press LTD.

routes: an incoming entangled polypeptide can have a distinctly different first-order rate constant for dissociation than the disentangled polypeptide.

Suppose that the first reaction in Scheme III is reversible (ATP + EP $\Leftrightarrow$ { ATP–E*}$_i$ + P) and transient low-affinity complexes, once formed, isomerize to stable complexes ({ATP–E*}$_i$$\rightarrow$ATP–E*). In this case, upon mixing ATP with DnaK–peptide complexes the intermediate complexes are subject to competing first- and second-order reactions: intermediate low-affinity complexes isomerize ({ATP–E*}$_i$ $\rightarrow$ ATP–E*) and peptide binding converts them back to high-affinity complexes ({ATP–E*}$_i$ + P $\rightarrow$ EP + ATP). Clearly, at low peptide concentrations, the isomerization reaction dominates, whereas at large peptide concentrations rebinding may be significant (Figs. 5 and 8). We therefore suggest that the high- to low-affinity structural switch in DnaK is bidirectional but that at low concentrations of peptide the switch appears to be unidirectional because the peptide-induced low- to high-affinity reaction is negligible.

COCHAPERONES

DnaJ is a 41-kDa cochaperone that together with GrpE (see below) enables DnaK to engage in repeated cycles of substrate binding and release. Homologues of DnaJ are found in eukaryotic cells [50]. Structural and functional details pertaining to DnaJ that are relevant to the understanding of the mechanism of action of 70-kDa chaperones are as follows. (i) DnaJ accelerates the rate of DnaK-catalyzed ATP hydrolysis in the steady state to the same extent as saturating concentrations of peptides [51], and a recent report has revealed that DnaJ can even accelerate the rate of DnaK-catalyzed ATP hydrolysis by a factor of 15,000 under single turnover conditions [52]; (ii) DnaJ and its homologues are composed of a "J" domain and a phenylalanine–glycine (Gly–Phe)-rich domain that are both required to stimulate chaperone-catalyzed ATP hydrolysis [53]; (iii) assorted polypeptides [54,55], including the low-affinity state of DnaK [56], bind to DnaJ, probably at the Gly–Phe-rich domain; and (iv) from single-turnover experiments, ATP appears to interact with DnaK–DnaJ (EJ) complexes according to

$$T + EJ \Leftrightarrow T\text{–}EJ \underset{k_{on}^{J}}{\overset{k_{off}^{J}}{\Leftrightarrow}} T\text{–}E^* + J$$

where T, E, and J denote ATP, DnaK, and DnaJ, respectively, and $k_{on}^{J} = 5.5 \times 10^4$ M^{-1} s^{-1} and $k_{off}^{J} = 0.24$ s^{-1} at 25°C [52]. This reaction is exactly analogous to Scheme II. The numerical value for k_{on}^{J} is similar to the numerical value of the second-order rate constant for the binding of the Cro peptide with low-affinity DnaK ($k_{on}^{Cro} = 2.4 \times 10^4$ M^{-1} s^{-1}), while the numerical value for k_{off}^{J} is about an order of magnitude smaller than the numerical value of the first-order rate constant for the dissociation of the Cro peptide from DnaK in the presence of ATP ($k_{off}^{Cro} = 3.3$ s^{-1}). On the basis of i–iv, one idea is that DnaJ first binds a polypeptide substrate and then "presents" the substrate to the low-affinity state of DnaK to form a transient macromolecular complex composed of DnaK, ATP, DnaJ, and the polypeptide substrate [51]. The low- to high-affinity conformational transition (TE* $\rightarrow$ TE) occurs as a consequence of this transient interaction between a low-affinity DnaK complex and a DnaJ–polypeptide complex, resulting in the capture of the polypeptide substrate in the binding site of the chaperone. The function of DnaJ may be to increase the affinity of a substrate to the low-affinity state of the chaperone by decreasing the magnitude of k_{off} for the substrate when it is bound to DnaJ (compare $k_{off}^{J} = 0.24$ s^{-1} to $k_{off}^{Cro} = 3.3$ s^{-1}). We propose that the binding of DnaJ or a DnaJ–polypeptide complex to low-affinity DnaK promotes the TE* $\rightarrow$ TE conformational change, and then the rapid

hydrolysis of DnaK-bound ATP occurs, consistent with reaction (5). As a result of these events the captured polypeptide substrate becomes part of a kinetically stable ADP–DnaK–substrate complex.

GrpE is a 22-kDa nucleotide exchange factor that binds as a dimer to a high-affinity ADP–DnaK–substrate complex and promotes the exchange of ATP for ADP [6,51,56–58]. Because ADP dissociates so slowly from DnaK this step must be catalyzed in order to tune the rate of the chaperone cycle to physiologic events that occur in the cell. Possibly, GrpE catalyzes a conformational transition in DnaK that occurs after the hydrolysis of ATP, as mentioned above (see The Low- to High-Affinity Transition ($E^* \rightarrow E$) with ATP Hydrolysis). GrpE catalyzes a 5000-fold acceleration in the rate of ADP release from DnaK [59]. When ATP binds to the DnaK–substrate–GrpE complex, GrpE dissociates. These two cochaperones have competing effects on DnaK: DnaJ shifts the high- to low-affinity equilibrium to the high-affinity state, which has a substrate tightly bound in the polypeptide-binding domain, whereas GrpE shifts the equilibrium to the low-affinity state, promoting the release of the bound substrate. Several studies have analyzed the effects of DnaJ and GrpE acting together on the activity of DnaK [51,56,60,61].

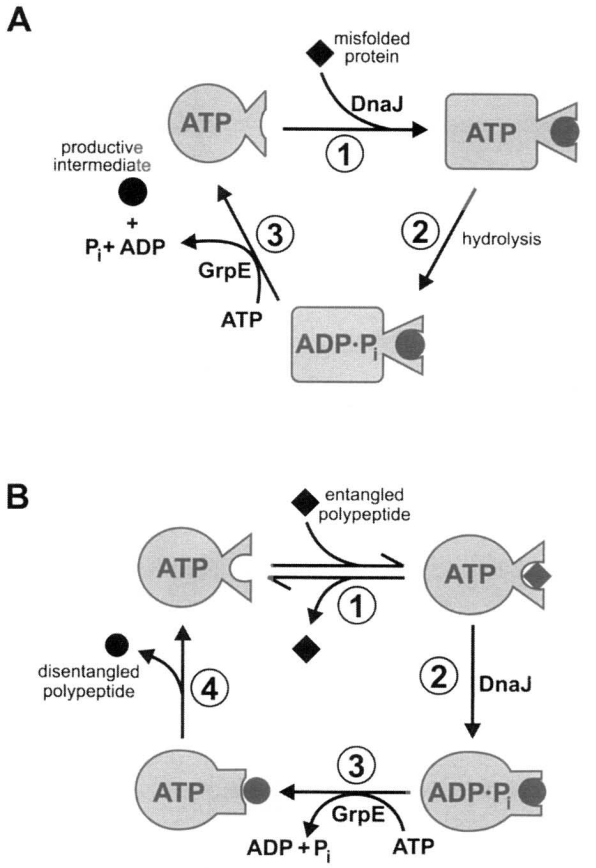

Fig. 9. **(A)** Chaperone reaction cycle based on Scheme II. (1) A misfolded substrate or aggregate binds to the low-affinity state, with assistance from the cochaperone DnaJ, and this binding induces the low- to high-affinity structural transition in DnaK. (2) ATP hydrolysis occurs, yielding a high-affinity DnaK–polypeptide complex. (3) The cochaperone GrpE binds to the high-affinity ADP–Dnak–peptide complex, catalyzing the release of ADP and binding of ATP, which in turn induces the high- to low-affinity structural switch and the expulsion of bound polypeptide. **(B)** Chaperone reaction cycle based on Scheme III. (1) A misfolded or entangled polypeptide reversibly binds to the low-affinity state. (2) DnaJ then binds to the low-affinity chaperone-polypeptide complex and catalyzes the hydrolysis of ATP, which in turn induces the low- to high-affinity structural switch. The conformation of the bound polypeptide also changes in this step, becoming more unfolded. (3) The cochaperone GrpE binds to the high-affinity ADP–Dnak–peptide complex, catalyzing the release of ADP and the binding of ATP, which in turn induces the high- to low-affinity structural switch to form an "activated" low-affinity intermediate complex. (4) The disentangled polypeptide is expelled from the polypeptide binding site of DnaK. Mechanism B was taken from Ref. 42 and printed with the permission of Academic Press LTD.

MODELS FOR THE 70-kDa CHAPERONE REACTION CYCLE

Two models for the 70-kDa chaperone reaction cycle are shown in Fig. 9. Similarities and differences between the two models are outlined below. In both models, the purpose of the interaction between the chaperone and the misfolded polypeptide substrate is to convert a misfolded substrate into a productive intermediate—this conversion may require several cycles of binding and release [56]—which then folds spontaneously (see Fig. 1). In our model, the conformational change in the polypeptide substrate occurs upon binding to the low-affinity state, whereas in the model of Gisler and co-workers the conformational change in the substrate is coupled to the hydrolysis of ATP by the chaperone [42]. Clearly, this is the most speculative part of the reaction cycle because of the paucity of experimental data.

Strong evidence has been found from fluorescence studies for the presence of a bidirectional conformational switch in 70-kDa chaperone molecules. The presence of this switch enables the rapid and complete release of diverse substrates, which may be bound to a chaperone molecule. It is important that substrates can be rapidly and completely released; otherwise the chaperone cycle would stall because the concentration of free chaperone would decline precipitously. There is intriguing evidence that the nucleotide exchange factor GrpE may even play a role in catalyzing the release of very tightly bound substrates from the chaperone [58]. Of course, the transi-

tion to the low-affinity chaperone state creates a problem: the binding of a nonnative polypeptide substrate to the low-affinity chaperone state is so weak that the reaction requires a catalyst. DnaJ is likely to be this catalyst. *In vivo*, the kinetics of the switch are regulated by the concentrations of ATP, polypeptide substrate, and cochaperones.

It is likely that several chaperone intermediates form during the reaction cycle in the presence of polypeptide substrates and cochaperones and that these intermediates are still uncharacterized. In our model of chaperone action (Fig. 9A), we expect that an intermediate forms transiently during each of the three steps depicted.

The linkage between ATP hydrolysis and the low- to high- affinity conformational switch is quite different in the two proposed models. In our model (Fig. 9A), the low- to high-affinity conformational switch is rate limiting and it precedes the hydrolysis of chaperone-bound ATP [reaction (5)]. The role of DnaJ is to catalyze substrate binding to the low-affinity chaperone state, which shifts the population of chaperone molecules from the low-affinity state to the high-affinity state. In contrast, in the model of Gisler and co-workers (Fig. 9B) [42], the hydrolysis of chaperone-bound ATP occurs in concert with the low- to high-affinity transition [reaction (3)]. DnaJ binding to a low-affinity chaperone–peptide complex catalyzes ATP hydrolysis and thereby accelerates the low-to-high-affinity transition. As can be seen from the two proposed models, the precise linkage between ATP hydrolysis and the low- to high-affinity conformational switch in the chaperone molecule is still controversial.

SUMMARY AND FUTURE DIRECTIONS

The mechanism whereby molecular chaperones carry out their diverse functions—protein folding, assembly, and transport—is the subject of intense investigations. Fluorescence-based kinetic studies have elucidated the mechanism of the ATP-induced conformational change in Hsp70 and Hsc70 proteins. Complementary structural studies are now needed to delineate the changes in chaperone architecture that occur as a consequence of both ATP binding and peptide binding. The molecular details of one of the most important aspects of the chaperone reaction cycle—ATP hydrolysis—and its coupling to the conformational change in the chaperone molecule are gradually emerging, but studies still are needed to clarify this aspect of chaperone function. In the future, experiments are needed to determine what change occurs in the polypeptide substrate molecule as a consequence of chaperone binding. Intriguing experiments might involve examining changes in the fluorescence of a DnaK-bound polypeptide using single-molecule fluorescence techniques.

ACKNOWLEDGMENTS

Support for this work came from NIH Grant GM51521. We thank Dr. Philipp Christen for letting us reprint figures from his publications.

REFERENCES

1. G. Becker and E. A. Craig (1994) *Eur. J. Biochem.* **219**, 11–23.
2. A. Bucherberger and B. Bukau (1997) in M.-J. Gething (Ed.), *Guidebook to Molecular Chaperones and Protein-Folding Catalysts*, Oxford University Press, Oxford.
3. W. J. Welch, D. K. Eggers, W. J. Hansen, and H. Nagata (1998) in A. L. Fink and U. Goto (Eds.), *Molecular Chaperones in the Life Cycle of Proteins*, Marcel Dekker, New York.
4. A. L. Fink and U. Goto (1998) in A. L. Fink and U. Goto (Eds.) *Molecular Chaperones in the Life Cycle of Proteins*, Marcel Dekker, New York.
5. B. Bukau and A. L. Horwich (1998) *Cell* **92**, 351–366.
6. S. Lindquist and E. A. Craig (1988) *Annu. Rev. Genet.* **22**, 631–677.
7. F. U. Hartl (1996) *Nature* **381**, 571–580.
8. D. Skowyra, C. Georgopoulos, and M. Zylicz (1990) *Cell* **62**, 939–944.
9. A. Ziemienowicz, D. Skowyra, J. Zeilstra-Ryalls, O. Fayet, C. Georgopoulos, and M. Zylicz (1993) *J. Biol. Chem.* **268**, 25425–25431.
10. D. R. Palleros, K. L. Reid, L. Shi, W. J. Welch and A. L. Fink (1993) *Nature* **365**, 664–666.
11. D. Schmid, A. Baici, H. Gehring, and P. Christen (1994) *Science* **263**, 971–973.
12. A. Buchberger, H. Theyssen, H. Schroder, J. S. McCarty, G. Virgallita, P. Milkereit, J. Reinstein, and B. Bukau (1995) *J. Biol. Chem.* **270**, 16903–16910.
13. K. L. Fung, L. Hilgenberg, N. M. Wang, and W. J. Chirico (1996) *J. Biol. Chem.* **271**, 21559–21565.
14. G. C. Flynn, T. G. Chappell, and J. E. Rothman (1989) *Science* **245**, 385–390.
15. S. Sadis and L. E. Hightower (1992) *Biochemistry* **31**, 9406–9412.
16. S. Blond-Elguindi, A. M. Fourie, J. F. Sambrook, and M.-J. H. Gething (1993) *J. Biol. Chem.* **268**, 12730–12735.
17. K. Park, G. C. Flynn, J. E. Rothman, and G. D. Fasman (1993) *Prot. Sci.* **2**, 325–330.
18. K. M. Flaherty, C. DeLuca-Flaherty, and D. B. McKay (1990) *Nature* **346**, 623–628.
19. K. M. Flaherty, D. B. McKay, W. Kabsch, and K. C. Holmes (1991) *Proc. Natl. Acad. Sci. USA* **88**, 5041–5045.
20. K. M. Flaherty, S. M. Wilbanks, C. DeLuca-Flaherty, and D. B. McKay (1994) *J. Biol. Chem.* **269**, 12899–12907.
21. J. C. A. Bardwell and E. A. Craig (1984) *Proc. Natl. Acad. Sci. USA* **81**, 848–852.
22. X. Zhu, X. Zhao, W. F. Burkholder, A. Gragerov, C. M. Ogata, M. E. Gottesman, and W. A. Hendrickson (1996) *Science* **272**, 1606–1614.
23. R. C. Morshauser, H. Wang, G. C. Glynn and R. P. Zuiderweg (1995) *Biochemistry* **34**, 6261–6266.
24. H. Wang, A. V. Kurochkin, Y. Pang, W. Hu, G. C. Flynn, and E. R. P. Zuiderweg (1998) *Biochemistry* **37**, 7929–7940.

25. S. J. Landry, R. Jordan, R. McMacken, and L. M. Gierasch (1992) *Nature* **355**, 455–457.
26. D. R. Palleros, W. J. Welch, and A. L. Fink (1991) *Proc. Natl. Acad. Sci. USA* **88**, 5719–5723.
27. D. R. Palleros, L. Shi, K. L. Reid, and A. L. Fink (1994) *J. Biol. Chem.* **269**, 13107–13114.
28. G. C. Flynn, J. Pohl, M. T. Flocco, and J. E. Rothman (1991) *Nature* **353**, 726–730.
29. S. Blond-Elguindi, S. E. Cwirla, W. J. Dower, R. J. Lipshutz, S. R. Sprang, J. F. Sambrook, and M.-J. H. Gething (1993) *Cell* **75**, 717–728.
30. A. Gragerov, L. Zeng, X. Zhao, W. Burkholder and M. E. Gottesman (1994) *J. Mol. Biol.* **235**, 848–854.
31. S. Rudiger, L. Germeroth, J. Schneider-Mergener, and B. Bukau (1997) *EMBO J.* **16**, 1501–1507.
32. L. E. Greene, R. Zinner, S. Naficy, and E. Eisenberg (1995) *J. Biol. Chem.* **270**, 2967–2973.
33. D. R. Palleros, K. L. Reid, J. S. McCarty, G. C. Walker, and A. L. Fink (1992) J. *J. Biol. Chem.* **267**, 5279–5285.
34. B. Banecki, M. Zylicz, E. Bertoli, and F. Tanfani (1992) *J. Biol. Chem.* **267**, 25051–25058.
35. S. M. Wilbanks, L. Chen, H. Tsuruta, K. O. Hodgson, and D. B. McKay (1995) *Biochemistry* **34**, 12095–12106.
36. L. Shi, M. Kataoka, and A. L. Fink (1996) *Biochemistry* **35**, 3297–3308.
37. R. Russell, R. Jordan, and R. McMacken (1998) *Biochemistry* **37**, 596–607.
38. J.-H. Ha and D. B. McKay (1995) *Biochemistry* **34**, 11635–11644.
39. B. Banecki and M. Zylicz (1996) *J. Biol. Chem.* **271**, 6137–6143.
40. H. Theyssen, H.-P. Schuster, L. Packschies, B. Bukau, and J. Reinstein (1996) *J. Mol. Biol.* **263**, 657–670.
41. S. V. Slepenkov and S. N. Witt (1998) *Biochemistry* **37**, 1015–1024.
42. S. M. Gisler, E. V. Peirpaoli, and P. Christen (1998) *J. Mol. Biol.* **279(4)**, 833–840.
43. S. V. Slepenkov and S. N. Witt (1998) *Biochemistry* **37**, 16749–16756.
44. C. D. Farr, F. J. Galiano, and S. N. Witt (1995) *Biochemistry* **34**, 15574–15582.
45. S. Takeda and D. B. McKay (1996) *Biochemistry* **35**, 4636–4644.
46. J. Zhang and G. C. Walker (1998) *Arch. Biochem. Biophys.* **356**, 177–186.
47. E. V. Pierpaoli, S. M. Gisler, and P. Christen (1998) *Biochemistry* **37**, 16741–16748.
48. D. R. Palleros, K. L. Reid, L. Shi, and A. L. Fink (1993) *FEBS Lett.* **336**, 124–128.
49. C. D. Farr, S. V. Slepenkov, and S. N. Witt (1998) *J. Biol. Chem.* **273**, 9744–9748.
50. D. M. Cyr, T. Langer, and M. G. Douglas (1994) *Trends Biochem. Sci.* **19**, 176–181.
51. R. Jordan and R. McMacken (1995) *J. Biol. Chem.* **270**, 4563–4569.
52. R. Russell, A. W. Karzai, A. F. Mehl, and R. McMacken (1999) *Biochemistry* **38**, 4165–4176.
53. A. W. Karzai and R. McMacken (1996) *J. Biol. Chem.* **271**, 11236–11246.
54. C. Alfano and R. McMacken (1989) *J. Biol. Chem.* **264**, 10699–10708.
55. J. Gamer, H. Bujard, and B. Bukau (1992) *Cell* **69**, 833–842.
56. A. Szabo, T. Langer, H. Schroder, J. Flanagan, B. Bukau, and F.-U. Hartl (1994) *Proc. Natl. Acad. Sci. USA* **91**, 10345–10349.
57. K. Liberek, J. Marszalek, D. Ang, C. Georgopoulos, and M. Zylicz (1991) *Proc. Natl. Acad. Sci. USA* **88**, 2874–2878.
58. C. J. Harrison, M. Hayer-Hartl, M. Di Liberto, F.-U. Hartl, and J. Kuriyan (1997) *Science* **276**, 431–435.
59. L. Packschies, H. Theyssen, A. Bucherberger, B. Bukau, R. S. Goody, and J. Reinstein (1997) *Biochemistry* **36**, 3417–3422.
60. E. V. Pierpaoli, E. Sanmeier, A. Baici, H.-J. Schönfeld, S. Gisler, and P. Christen (1997) *J. Mol. Biol.* **269**, 757–768.
61. E. V. Pierpaoli, E. Sandmeier, H.-J. Schönfeld, and P. Christen (1998) *J. Biol. Chem.* **273**, 6643–6649.